Energy and Mass Balance of Forni Glacier (Stelvio National Park, Italian Alps) from a Four-Year Meteorological Data Record

Authors: Senese, Antonella, Diolaiuti, Guglielmina, Mihalcea, Claudia, and Smiraglia, Claudio

Source: Arctic, Antarctic, and Alpine Research, 44(1) : 122-134

Published By: Institute of Arctic and Alpine Research (INSTAAR), University of Colorado

URL: https://doi.org/10.1657/1938-4246-44.1.122

Arctic, Antarctic, and Alpine Research, Vol. 44, No. 1, 2012, pp. 122–134

Energy and Mass Balance of Forni Glacier (Stelvio National Park, Italian Alps) from a Four-Year Meteorological Data Record

*Antonella Senese**† *Guglielmina Diolaiuti**‡ *Claudia Mihalcea**§ *and Claudio Smiraglia**¶

*Università degli Studi di Milano, Department of Earth Sciences (A. Desio), Via Mangiagalli 34, 20133 Milan, Italy
†Corresponding author: antonella.senese@unimi.it
‡guglielmina.diolaiuti@unimi.it
§claudia.mihalcea@unimi.it
¶claudio.smiraglia@unimi.it

Abstract

Since 26 September 2005 an Automatic Weather Station (AWS1 Forni) has been running on the ablation area of the largest Italian valley glacier, Forni, in the Ortles–Cevedale Group. A 4-year record (from 1 October 2005 to 30 September 2009) of air temperature, relative humidity, wind speed and direction, incoming and outgoing radiative fluxes, air pressure, liquid precipitation, and snow depth is considered. The meteorological data are analyzed to describe glacier surface conditions, to calculate the energy balance, and to evaluate the ice ablation amount. Snow accumulation was measured, thus permitting the estimation of the glacier point mass balance.

An annual average amount of melt of -5.4 ± 0.021 m w.e. was calculated and an annual average amount of accumulation of $+0.7 \pm 0.006$ m w.e. was measured at the AWS site. The annual average amount of mass balance was -4.7 ± 0.023 m w.e.

Our analyses show that surface conditions during summer and fall seasons are important in regulating glacier albedo and then mass balance. In particular, snow cover presence, due to a longer persistence of spring snow, summer snowfalls and earlier fall solid precipitation, drives the duration of the ice melt period.

http://dx.doi.org/10.1657/1938-4246-44.1.122

Introduction

Changes in climatic forcing are directly reflected by the mass budget of snow and ice surfaces (von Hann, 1897; Hock, 2005). Understanding the impact of changing climate conditions on glacier melt is a prerequisite for projections of glacier volume changes which are needed to study mountain hydrology, to analyze natural hazard frequency, and to forecast sea level rise. In recent years, numerical models have been frequently used to study the properties of individual glaciers and ice caps, to understand their fluctuations in history, and to make projections of future behavior for imposed climate scenarios (e.g. Gregory and Oerlemans, 1998; Oerlemans et al., 1998). The numerical approach embraces both glacier ice-flow and mass-balance models. The latter translate meteorological conditions into glacier mass balance. The general experience from numerical studies (Wallinga and van de Wal, 1998; Oerlemans, 2000) confirms that uncertainties in the mass-balance models are strongly reflected in the output. Then, to improve ice-flow modeling and glacier projections it is important to refine the calculation of the glacier mass balance. A general problem in testing and calibrating mass-balance models is the scarceness of meteorological data from glaciers.

The glacier surface differs from its surroundings during the ablation season due to surface characteristics. Low surface temperature and varying albedo conditions characterize the glacier surface, while external mountain slope areas, with no snow cover during summer, present lower albedo of rock surfaces, which warm faster than the glacier surface during the day. The surface energy balance of lateral slopes is higher and influences the nearby glacier surface through increased outgoing longwave radiation flux and air temperature. The differences are minimized during the winter season and in the accumulation area due to snow cover distribution, reflecting more than 50% of the incoming shortwave radiation due to a high albedo. Therefore, to calculate the glacier energy balance, direct measurements of energy fluxes at the interface between the atmospheric boundary layer and glacier surface are necessary (Greuell and Oerlemans, 1986).

An important question to be answered is how the atmospheric boundary layer overlying a glacier filters the large-scale climatic signal. Especially when the glacier surface is melting and the air is warm, a boundary layer with special properties is present (e.g. Munro, 1989; van den Broeke et al., 1994; Greuell et al., 1997). The structure of the atmospheric boundary layer over the glacier influences the surface energy budget by controlling the latent and sensible turbulent heat fluxes. The glacier winds generate turbulence in the stably stratified surface layer and are especially well developed during periods with weak synoptic flow and strong insolation, enhancing the melt rates. In the accumulation zone, where the temperatures are lower and the surface-layer stratification is unstable (except during summer), the atmospheric boundary layer is more sensitive to external forcing, such as the valley wind, transporting moist and warm air from the valley floor. The pronounced mass flux divergence within the lower parts of the atmosphere during the night, caused by the combined effect of the glacier and mountain wind, produces drying and warming of the atmospheric boundary layer air (van den Broeke, 1997). Turbulent cooling of the air by the melting ice surface results in a down-glacier directed flow component.

From these considerations, it is clear that ground measurements of the meteorological parameters on glaciers are very useful. Systematic investigations of the heat budget of a melting glacier did not start until after the Second World War. Pioneering work was done by Capello (1959–1960) and Ambach (1963). A series of other investigations followed (e.g. Björnsson, 1972; Hogg et al., 1982; Ishikawa et al., 1992), and these studies have given basic insight into the nature of the energy budget on glaciers. In recent

1523-0430/12 $7.00

decades, glacio-meteorological experiments have been carried out, and the components of the surface energy flux were measured simultaneously at a large number of automatic weather stations (AWSs) (Oerlemans and Vugts, 1993; Greuell et al., 1997; Oerlemans et al., 1999). Large data sets have been obtained, providing insight into altitudinal gradients of meteorological quantities and improving glacier melt modeling (Munro and Marosz-Wantuch, 2009). Also, on debris-covered glaciers, meteorological data and energy fluxes have been collected by installing seasonal AWSs (Brock et al., 2010). Most of the studies provided supraglacial meteorological data and energy fluxes measurements for shorter periods (one or more ablation seasons). However, longer records of data are needed to calculate the annual energy and mass balance and these can only be obtained from AWSs permanently located at the glacier surface.

Most AWSs are located in the accumulation zone, due to the higher stability, whereas only a few are present in the glacier ablation area. The main reason is the high melt rates in the ablation area, which compromise the stability of the AWSs at the glacier surface during the ablation season. Dynamic supraglacial morphologies and crevasses characterizing the ablation area also represent a problem. From 1987 several permanent AWSs have been located on the glacier ablation areas. To set up the AWSs, structures (a mast with four legs) able to stay freely on the ice surface and to adjust to the melting surface are used. This allowed the installation of AWSs designed to provide data all year round on the melting zones of the Greenland Ice Sheet, of Hardangerjokulen (Norway), and of the Morteratschgletscher (Switzerland) (Oerlemans, 2000; Oerlemans and Klok, 2002; Klok and Oerlemans, 2004). Up to now the longest glacier data series was obtained from the AWS located on the Morteratschgletscher (Switzerland). Due to the possibility of regular visits and to the favorable atmospheric conditions (little icing), a good quality meteorological data set was obtained during the last 2 decades (Oerlemans, 2001, 2009). The Morteratschgletscher AWS was used as a valuable example for the installation of the first Italian permanent AWS on the ablation area of Forni Glacier, in the Alps (Citterio et al., 2007).

On the Italian Alpine glaciers, a long tradition of field surveying is present: length variation and mass-balance measurements started, respectively, in 1895 at Forni Glacier (Lombardy) and in 1967 at Careser Glacier, (Trentino) (Smiraglia, 2003). Nevertheless, continuous monitoring of long-term meteorological data, energy fluxes measured directly at the glacier surface, and energy balance studies are still lacking. During the last decades, the Italian AWSs (collecting data during different periods) were located in glacierized areas on rock exposures, nunataks, or buildings (such as mountain huts), thus making the meteorological data representative of high mountain atmospheric conditions but not very useful for analysis of the supraglacial micrometeorology. The first permanent Italian AWS on a glacier ablation area was installed on Forni Glacier on 26 September 2005. The aims were to collect meteorological data, to measure the energy fluxes at the glacier/atmosphere interface, to calculate energy available for the ice ablation, and to measure the snow accumulation. The Forni AWS results are also interesting for comparison with the AWS located on the Morteratsch Glacier managed by Institute for Marine and Atmospheric Research Utrecht (IMAU). Forni and Morteratsch glaciers are situated on the south side and north side, respectively, of the Alps—both with north aspect and similar geometry settings. The main differences between the two AWS locations are: the AWS Forni is about 500 m higher than AWS Morteratsch (Oerlemans, 2001), Morteratsch Glacier has a larger area (16 km^2) than the Forni Glacier (12 km^2), and the Forni site is dryer (i.e.: less precipitation and lower relative humidity values) (Table 1).

TABLE 1

Comparison between Forni and Morteratsch Glacier: site characteristics, meteorological and energy balance data. Morteratsch Glacier data are annual mean values of 2000, except the albedo which is the mean value of 1995.

	Forni Glacier	Morteratsch Glacier
Coordinates	46°23′56″N; 10°35′25″E	46°24′34″N; 9°55′54″E
Elevation range (m a.s.l.)	2600–3670	1900–4049
Length (km)	3	7
Area (km^2)	12	16
AWS elevation (m a.s.l.)	2631	2100
net SW (W m^{-2})	68	67
net Lw (W m^{-2})	−38	−36
SH (W m^{-2})	18	36
LE (W m^{-2})	−5	6
R_S (W m^{-2})	36	76
SW in (W m^{-2})	151	136
SW out (W m^{-2})	91	72
SW in extra-terrestrial (W m^{-2})	267	292
Air temperature (°C)	−1.3	2.1
Snow albedo	0.85	0.75
Ice albedo	0.35	0.35

In this paper a 4-year record of hourly meteorological data (from 1 October 2005 to 30 September 2009) measured in the ablation area of Forni Glacier, is analyzed with the aims of describing glacier surface conditions, evaluating the surface energy and mass exchanges, and analyzing a new data set of meteorological observations obtained over the melting Forni Glacier surface to investigate processes and surface characteristics which are driving the surface energy balance. The focus is energy and mass-balance calculation and the sensitivity to the albedo and the conditions in which melting and condensation occur. The availability of humidity, air pressure, and wind velocity data permits a more accurate calculation of turbulent fluxes than other studies (i.e. Oerlemans, 2000; Klok and Oerlemans, 2002). The study represents a further development of the previous paper by Citterio et al. (2007), which dealt with 1 year of meteorological data. The analysis of interannual variability of the energy and mass balance estimations is performed. Then we compare our results on Forni Glacier to previous studies on different glacier sites (e.g. Morteratsch Glacier, Switzerland). The influence of surface albedo variability on ice melting is evaluated to analyze and discuss the parameters influencing the surface energy budget of an alpine glacier. Furthermore the energy and mass-balance results from our study contribute to the evaluation of the meltwater discharge from the Forni Glacier basin, in Stelvio National Park. This is particularly important as Forni meltwater is also utilized for hydropower production.

The AWS1 Forni

The Automatic Weather Station Forni (AWS1 Forni) is set up on the ablation tongue at the base of the eastern icefall of Forni Glacier. Forni is the largest Italian valley glacier (surface area of about 12 km^2), and is situated in the Ortles–Cevedale Group, Stelvio National Park, Lombardy Alps. The glacier is about 3 km long (Fig. 1), has a northward down-sloping surface, and stretches over an elevation range of 2600 to 3670 m a.s.l. The WGS84 coordinates of AWS1 Forni are: 46°23′56.0″N (46.40°N), 10°35′25.2″E (10.60°E), 2631 m a.s.l. (Fig. 1). The AWS location

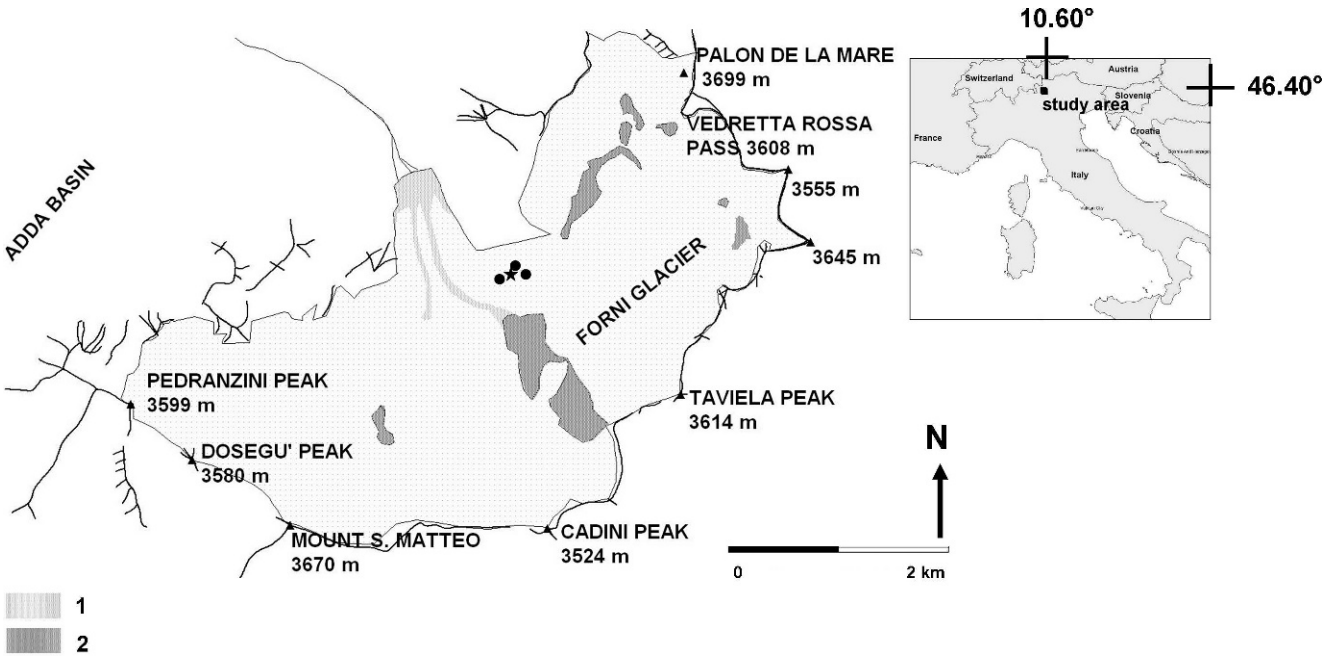

FIGURE 1. Location (black star) of the AWS1 Forni and the three ablation stakes (black dots); the AWS and the ablation stakes are located in an area of about 50 m^2. The light gray areas are used to mark supraglacial debris coverage, the dark gray areas are used to indicate rock exposures and nunataks.

is a good compromise between the need to minimize local topographical effects (almost flat surface and absence of crevasses) and to decrease the probability of snow avalanches during winter in the AWS vicinity. The AWS is positioned on the lower glacier sector, at 800 m from the glacier terminus.

The AWS was installed on 26 September 2005. In the following years the AWS was checked several times, particularly during the first year, without any problem being observed (Citterio et al., 2007). The AWS is equipped with sensors (Table 2, Fig. 2) for measuring air temperature and humidity (naturally ventilated sensor), wind speed and direction, air pressure, and the four components of the radiation budget (longwave in and out, solar in and out). A 1000 cm^2 unheated rain gauge and a Campbell SR-50 sonic ranger are also set up to measure, respectively, rain and snow depth. The whole system is supported by a four-leg, 5-m-high stainless steel mast standing on the ice surface according to the construction and setting proposed and tested by IMAU (Oerlemans, 2001). The AWS stands freely on the ice, and adjusts to the melting surface during summer. Supraglacial morphologies (bedières) may develop at the AWS location, which can compromise the stability. In this case the AWS needs to be moved to a more stable surface. The height where instruments are placed was chosen in order to permit their activity also during the wintertime when snow covers the glacier surface and partially buries the AWS mast.

The sonic ranger is installed on the AWS mast, measuring only the accumulation and not the ice ablation. An important feature of the thermo-hygrometer is the radiation shield with natural ventilation, thus permitting an air flow around the sensor, limiting the error due to radiation overheating. Due to the naturally ventilated sensor our air temperature measurements could be overestimated (up to a few degrees) during high radiation/low wind speed conditions (Georges and Kaser, 2002); on the other hand, such conditions seem to be dominating only during limited periods (early spring). The albedo values during snowfall events are overestimated due to snow presence on the upfacing pyranometer. To solve this problem, the values affected by the overestimations were filtered and not considered in our analysis. No problems of rime ice accumulation on instruments were observed during the 4 years of data collection, based on the analysis of wind speed and direction data (which are consistent over the entire period).

TABLE 2

Sensor and data logger specifications installed at the AWS1 Forni.

Variable	Range	Accuracy	Recording rate	Height	Manufacturer
Data logger				1.5 m	LSI-Lastem Babuc ABC
Air temperature	−30 to +70 °C	± 0.001 °C	30 min.	2.6 m	LSI-Lastem DMA570
Relative humidity	0–100%	± 1%	30 min.	2.6 m	LSI-Lastem DMA570
Air pressure	400–800 hPa or mBar	± 10 hPa	60 min.	1.5 m (inside the logger box)	LSI-Lastem DQA223
Solar radiation	0.3–3 μm	± 5% of the value	30 min.	3.17 m	Kipp and Zonen CNR-1
Infrared radiation	5–50 μm	± 5% of the value	30 min.	3.17 m	Kipp and Zonen CNR-1
Snow level	0–1000 cm	± 2 cm	60 min.	3.17 m	Sonic Ranger Campbell SR50
Liquid precipitation	0–1000 mm	± 1 mm	30 min.	4 m	LSI-Lastem DQA035
Wind speed	0–50 m s^{-1}	± 1%	60 min.	5 m	LSI-Lastem DNA022
Wind direction	0°–360°	± 1°	60 min.	5 m	LSI-Lastem DNA022

FIGURE 2. AWS1 Forni. The instruments are marked with numbers: (1) wind speed and direction, (2) rain gauge, (3) net radiometer CNR1, (4) sonic ranger, (5) thermo-hygrometer, (6) solar panels, and (7) barometer inside the datalogger box (photo by G. Diolaiuti).

Power is supplied by two solar panels (40 Watt) and a lead-gel battery; the battery voltage over time is recorded by the datalogger. The battery-only power supply in the present configuration is estimated in excess of 2 months, with the solar panels permanently obscured by snow accumulation and accounting for low temperature operation and self discharge. Data points, sampled at 60-second intervals and averaged over a 30-minute time period for most of the sensors (see the fourth column in Table 2), are recorded in the flash memory card, including the basic distribution parameters (minimum, mean, maximum, and standard deviation values). Wind data are sampled every 5 seconds, and then processed to obtain an hourly data set of information, including minimum, maximum and average speed, and dominant wind direction.

Methods

AWS1 Forni has been running continuously since its installation with only one interruption between 5 and 11 October 2008. In this study we analyze and compare 4 hydrological years (for the hydrological year we consider the period from 1 October to 30 September of the next year). All the annual values are averaged on the hydrological year basis.

SOLID PRECIPITATION

Snowfall measurements provide important information for evaluating glacier accumulation and thus mass balance. Forni Glacier is one of the sites frequently monitored by *Centro Nivometeorologico di Bormio* of the Lombardy Regional Agency for Environmental Protection (*ARPA Lombardia*); therefore, it is possible to compare the collected snow pit data to the data record from the sonic ranger of the AWS1 Forni. Comparison of the two data sets confirms the reliability of the data acquired by the sonic ranger over one year of data (Citterio et al., 2007). In our analysis we use a 140 kg m^{-3} fresh snow density and, to distinguish snowfall from liquid precipitation, a +1.5 °C temperature threshold value (Hock, 1999; Klok and Oerlemans, 2002; Huss et al., 2009; Paul et al., 2009).

RADIATION

To calculate the surface energy balance, the hourly radiation data were analyzed. At the glacier surface, solar radiation is the most important energy balance component driving ice and snow melt. Therefore the albedo (from here α) is an important and noteworthy parameter of glacier surface to be analyzed in terms of temporal variability.

Firstly, we filtered the incoming and outgoing shortwave radiation data (SW_{in} and SW_{out}, respectively) in order to remove erroneous values (e.g.: after a snowfall event, values showing SW_{out} exceeding SW_{in} due to the presence of fresh snow on the top pyranometer); then the following relation was applied:

$$\alpha = SW_{out} * SW_{in}{}^{-1} \quad (1)$$

The incoming and outgoing longwave radiation (LW_{in} and LW_{out}, respectively), were measured by the CNR1 pyrgeometers. The acquired data represent the flux at each sensor surface, and the values have been converted to the ground and atmospheric (upward and downward) directional flux by Stephan-Boltzmann's law.

TURBULENT FLUXES

Because measurements are available for one level only, no attempt was made to use sophisticated schemes for the calculation of the turbulent heat fluxes. Instead, the well-known bulk aerodynamic formulas were used according to the methods introduced by Oerlemans (2000):

$$SH = \rho_a * c_p * C_h * V_{2m} * (T_{2m} - T_S) \quad (2)$$

$$LE = 0.622 * \rho_a * L_v * C_h * V_{2m} * (e_{2m} - e_S) * p^{-1}, \quad (3)$$

where ρ_a is air density (0.87 kg m^{-3}), c_p is the specific heat of dry air (1.006 kJ kg^{-1} $°C^{-1}$), C_h is the turbulent exchange coefficient (0.00127 ± 0.00030; from Oerlemans, 2000), V_{2m} is the wind speed value at 2 m, T_{2m} is the air temperature value at 2 m, T_S is the surface temperature, L_v is the latent heat of vaporization (Harrison, 1963), e_{2m} is the vapor pressure value at 2 m, e_S is the vapor pressure value at the surface (calculated using the Wexler formula; Wexler, 1976) and p is the air pressure value at sensor level. The T_S is calculated by using the Stephan-Boltzmann law: $T_S = \sqrt[4]{(LW_{out} * \sigma^{-1} * \varepsilon^{-1})}$, where σ is the Stephan-Boltzmann constant, $5.67 * 10^{-8}$ W m^{-2} K^{-4}, and ε is the emissivity of the snow/ice surface, assumed to be equal to unity. Wind speed and air temperature and humidity are measured at 5 m and 2.6 m, respectively, then they are calculated at 2 m (following the method introduced by Oerlemans, 2000). The C_h is assumed to be constant, because no information on how roughness lengths change during the year is available (Oerlemans and Klok, 2002).

An overestimation of the turbulent fluxes calculations may occur in spring due to overestimation of air temperature under low wind/high global radiation conditions.

The outgoing longwave flux at the glacier surface cannot exceed the flux for a melting surface, which is about 316 W m^{-2}. However, since the sensor is installed at a height of about 3.17 m, we can assume a contribution from the air layer between the surface and the sensor. The measured flux can therefore be slightly larger than 316 W m^{-2} (Oerlemans, 2009); in these cases the surface temperature is set to 0 °C (Oke, 1987; Oesch et al., 2002; Mölg and Hardy, 2004; Pellicciotti et al., 2008; Rupper and Roe, 2008).

SURFACE ENERGY AND MASS BALANCE

To calculate the glacier energy and mass-balance components, we applied the following methods by considering the hourly meteorological values. The energy balance at the glacier surface (R_S) determines the net energy available for heating and melting. R_S was calculated as

$$R_S = SW_{net} + LW_{net} + SH + LE. \quad (4)$$

All the fluxes (W m^{-2}) were defined positive when directed towards the surface. The conductive heat flux at the surface was neglected since no temperature sensors were located in the snowpack and in the ice surface layer. During the ablation season (i.e. from June to October), when melting occurs and surface ice temperature is ~0 °C, all the energy is used at the glacier surface to melt the ice. Consequently, the conductive heat flux at the surface is equal to zero, thus permitting the calculation of R_S without considering it. In contrast, when the glacier surface is not at the melting point (i.e.: from October to June) and R_S is lower than 0 W m^{-2}, the surface cools and the conductive heat flux value is not equal to zero and has to be evaluated. In our study, neglecting the conductive heat flux at the surface results in a slight overestimation of ice melting.

The glacier annual mass balance is the sum of accumulation and ablation (i.e.: mass gain and loss, respectively) over a one-year-long period. On Forni Glacier the main ablation process is the surface melting, which occurs from late spring to early fall. At this time we focused on the ice and snow melting (M) calculation from the glacier energy balance. The negative M value was added to the snow accumulation (P_{solid}) positive value, thus giving the specific annual mass balance (B) at the location of the AWS1 Forni.

The ablation amount (M) was obtained from:

$$M = -R_S * {L_m}^{-1}, \quad (5)$$

where M is the rate of change of mass (kg m^{-2} or mm w.e.), L_m is the latent heat of melting (3.34×10^5 J kg^{-1}). It is assumed that melting occurs as soon as the surface temperature is at 0 °C and R_S is positive.

The accumulation amount was calculated considering daily fresh snow values recorded by the sonic ranger. To convert accumulated fresh snow into water equivalent, a density of 140 kg m^{-3} was used to obtain the solid precipitation value (P_{solid}).

Finally the mass balance (B) was calculated as

$$B = \int_0^T (M + P_{solid})dt, \quad (6)$$

where t is the time we analyzed during the 4-year period (from 0 to T, that is from 00:00 a.m. on 1 October 2005 to 11:00 p.m. on 30 September 2009). The calculation is made also on an annual basis (from 1 October to 30 September of the next year).

Results

METEOROLOGY

The data collected by the AWS1 Forni are summarized in Figure 3. Daily average values of wind speed, air temperature, global radiation and clear-sky global radiation, albedo, snow depth, and accumulated fresh snow are shown. In general, wind speed values were low (Fig. 3, part a): a 4-year mean value of 4.99 m s^{-1} was found. Nevertheless, daily maxima up to 17 m s^{-1} were registered (e.g.: 17.03 m s^{-1} on 6 September 2007) and maximum hourly values exceeded 25 m s^{-1} (e.g.: 25.11 m s^{-1} on 27 January 2008 at 10:00 a.m.). By analyzing the hourly data, the low wind speed values (lower than 1.5 m s^{-1}) or calm state (0 m s^{-1}) account for 9% over the entire period (1% of calm state) on Forni Glacier, thus minimizing the air temperature overestimations.

Daily mean values of air temperature are shown in Figure 3 (part b). From the analysis of all the daily mean temperature data, an annual diagram was obtained with an expected annual cycle (maxima occurring in the summer and minima during winter). Over the 4-year period an average air temperature of −1.3 °C was found, and the annual range was typically 7.4 °C. Regarding the extreme mean daily values, the AWS measured −22.9 °C in winter (29 December 2005) and +11.1 °C in summer (25 June 2008).

Figure 3 (part c) shows the global radiation trend. An interesting feature is the increase in the daily variability in spring, which is due to the increasing potential incoming shortwave radiation. This increases the contrast between clear days (high values) and cloudy days (low values). This feature, observed also on Morteratschgletscher, seems to be enhanced by the disappearance of snow cover on the sides of the glacier valley, reducing the effect of multiple reflection over the glacier surface (Oerlemans, 2000). A mean global radiation of 151 W m^{-2} was measured. A comparison with the annual mean extraterrestrial irradiance, calculated for the same latitude and elevation and equal to 267 W m^{-2}, makes clear that shading and clouds strongly decrease the amount of solar energy at the glacier surface. The reduction is ca. 44% excluding the processes of scattering and absorption of the clear atmosphere.

The mean 4-year albedo value (Fig. 3, part d) is 0.65. During the accumulation season, the 4-year mean annual albedo value was 0.85 while during the ablation season, the mean annual value was 0.35. This shows a marked seasonal cycle related to the different surface reflectivity between ice and snow (Table 3). In fact, a snowfall implies higher albedo, increasing outgoing radiation and less energy available for melting.

The last two panels of Figure 3 (parts e and f) present the snow data. In panel e, snow depth (m) is measured at the sonic ranger. A large annual variability is seen. To underline the correlation between snow depth and accumulated fresh snow, in the last panel the yearly fresh snow accumulation (with a density of 140 kg m^{-3}) is represented. Comparing these two parameters, higher values of snow depth are related to the higher amounts of fresh snow (e.g. in 2009).

ENERGY BALANCE

The components of the glacier surface energy balance are summarized in Figure 4. Daily mean values are characterized by

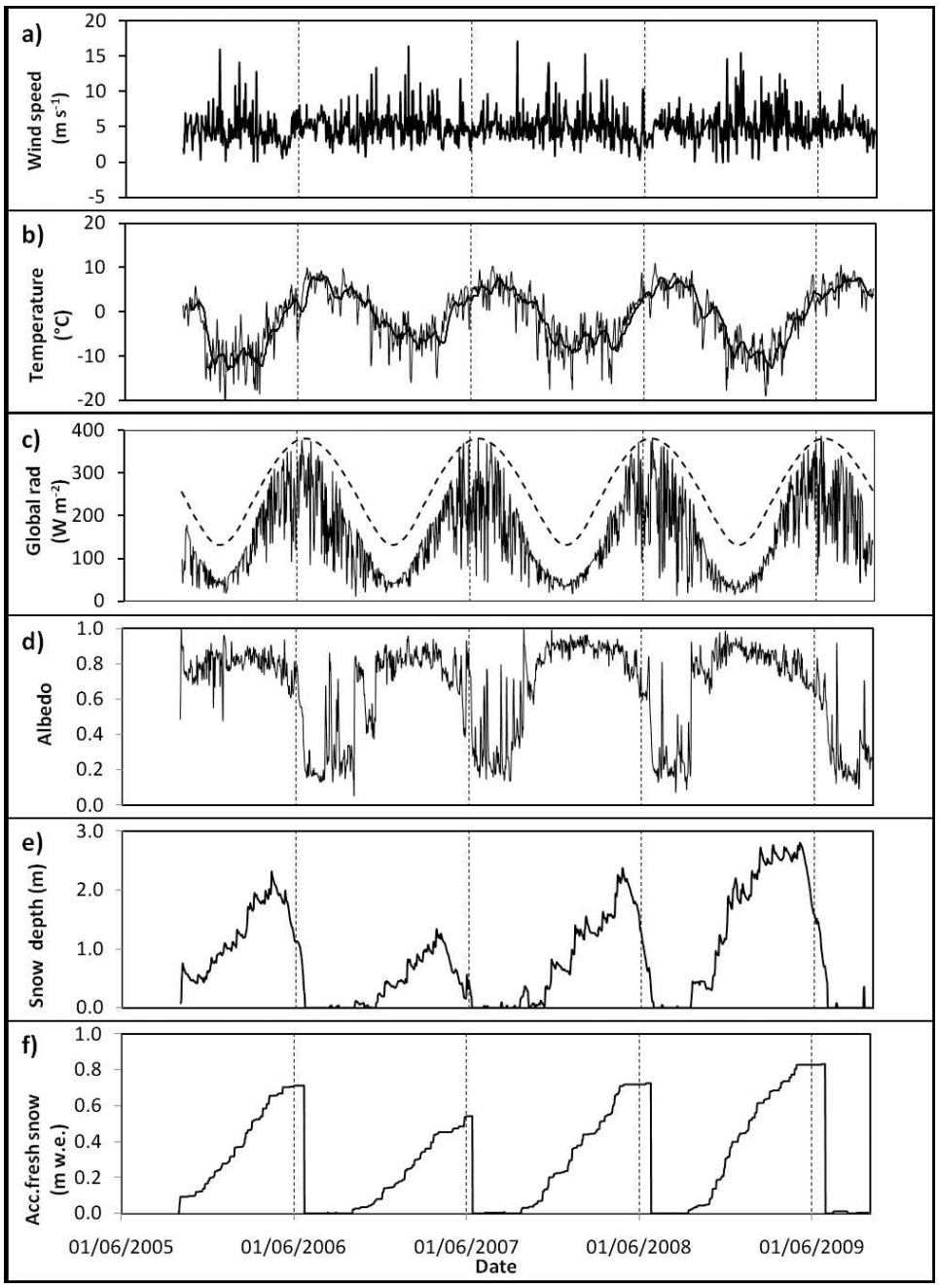

FIGURE 3. Daily mean values of (a) wind speed; (b) air temperature; (c) global radiation (solid curve) and clear-sky global radiation (dashed curve); (d) albedo; (e) snow depth (m); and (f) accumulated fresh snow (m w.e.) for the entire period, from 1 October 2005 to 30 September 2009. The dates shown are dd/mm/yyyy.

similar trends of the annual cycle over the analysis period (from 1 October 2005 to 30 September 2009); all the maximum values occur during summer, and all minimum during winter except the values of net longwave radiation. In particular, the net shortwave radiation shows maxima during the summer (ranging from 250 W m^{-2} to 300 W m^{-2}) and minima during winter (with values near 0 W m^{-2}); net longwave data vary between slightly positive values (close to 0 W m^{-2}) and negative values (up to -100 W m^{-2}, realistic values due to the 0 °C glacier surface). Daily LW average values are rarely positive, and usually slightly positive values occur only during warm and not too cloudy summer days. The sensible heat flux is generally positive and exceeds the latent heat flux. The latent heat flux is generally positive during the ablation season, but during the rest of the year is negative due to low humidity in combination with a minimal temperature difference between the surface and the air (Oerlemans, 2000). A similar trend is found for the net energy (R_S) diagram with maxima of ca. 300 W m^{-2} and minima of ca. -100 W m^{-2}. The negative values characterize the winter periods, when ice melting is absent. The increase in net energy is very steep in late spring/early summer due to the transition from a snow-covered to a bare ice surface. The transition from bare ice to snow cover in October/November is more gradual, because then the incoming shortwave radiation flux is reduced. Analyzing the annual mean values of all parameters, the year 2007/2008 is characterized by a lower net SW and R_S; in contrast, the year 2008/2009 is dominated by a higher net SW, net LW, and LE. The highest R_S is calculated in 2005/2006 with intermediate values of net SW, net LW, and LE.

Filtering surface temperature (T_S), net energy (R_S), and latent heat flux (LE) data, the hours when melting (i.e.: when $T_S = 0$ °C and $R_S > 0$ W m^{-2}) and condensation (when $T_S = 0$ °C and LE >

TABLE 3

Comparison of cumulative melting, solid precipitation, mass balance, net shortwave radiation, and mean energy balance, air temperature and albedo annual values (from 1 October of the year x to 30 September of the year x+1) and meteorological seasons (meteorological fall from 1 September to 30 November; meteorological winter from 1 December to 28/29 February; meteorological spring from 1 March to 31 May; meteorological summer from 1 June to 31 August).

Hydrological year	Cumulative melting (m w.e.)	Cumulative solid precipitation (m w.e.)	Cumulative mass balance (m w.e.)	Mean albedo	Mean energy balance (W m^{-2})	Cumulative net shortwave radiation (MJ)	Mean air temperature (°C)
2005/2006	−5.6 ± 0.021	+0.7 ± 0.006	−4.9 ± 0.023		42	2244	−2.1
fall				0.77	−16	128	−2.6
winter				0.82	−19	105	−10.4
spring				0.78	16	439	−3.1
summer				0.34	153	1270	5.1
2006/2007	−5.5 ± 0.020	+0.6 ± 0.005	−4.9 ± 0.021		35	2228	−0.2
fall				0.51	18	470	1.5
winter				0.82	−21	101	−5.7
spring				0.76	13	499	−1.1
summer				0.33	150	1208	5.6
2007/2008	−5.0 ± 0.021	+0.7 ± 0.006	−4.2 ± 0.023		33	1886	−1.3
fall				0,70	−12	395	−1.4
winter				0.90	−31	51	−6.8
spring				0.84	7	334	−3.0
summer				0.34	162	1240	5.9
2008/2009	−5.6 ± 0.020	+0.8 ± 0.007	−4.8 ± 0.023		40	2180	−1.5
fall				0.71	0	226	−1.2
winter				0.87	−27	77	−9.6
spring				0.78	16	543	−2.0
summer				0.37	156	1238	5.9

0 W m^{-2}) are found (Fig. 5). Considering only these hours, which accounts for about 31% for melting and about 24% for condensation, SW_{net}, LW_{net}, SH, LE, and R_S are averaged. By analyzing these mean values, the net shortwave proves to be the parameter with the highest energy flux during both melting and condensation conditions (with values of 176 W m^{-2} and 123 W m^{-2}, respectively). Moreover, some differences are found: during melting, R_S is higher than during condensation; during melting the net longwave reaches values of −24 W m^{-2}, but during condensation −20 W m^{-2}. The latent heat flux value is higher during condensation (12 W m^{-2}) than during melting (4 W m^{-2}). Sensible heat flux value is similar in both situations (ca. 30 W m^{-2}).

MASS BALANCE

The solid precipitations curve (Fig. 3, part f) is characterized by a stepwise increase during the winter period and quite stable conditions during the summer period when only a few snowfalls occur. In fact, when the ablation processes dominate, the air temperature is warmer and solar radiation influence is higher. The total accumulation during the 4 years was +2.8 m w.e. The maximum value is registered during 2008/2009 (Table 3), characterized by heavier snowfalls (+0.8 ± 0.007 m w.e.). An intermediate total yearly value of +0.7 ± 0.006 m w.e. is measured during 2005/2006 and 2007/2008, whereas 2006/2007 is characterized by the minimum value (+0.6 ± 0.005 m w.e.).

Figure 6 shows the cumulative ablation and mass balance curves over the entire period. The melt is calculated from the complete energy balance and considering only melting hours. A total melt value of −21.6 kg m^{-2} or m w.e. was calculated. The annual values are presented in Table 3. The highest losses occurred during 2005/2006 and 2008/2009, but instead less ablation characterizes 2007/2008.

Analyzing daily values of mass balance (Fig. 7), we can observe how the mass losses prevail over gains. The accumulation does not exceed +0.05 m w.e. day^{-1} and the ablation values reach up to −0.09 m w.e. day^{-1}. Moreover, the cycle of surface mass balance is shown: during winter the melting is absent, instead it dominates during ablation season (June–October). This cycle is evident also from analyzing the cumulative curve (Fig. 6); in fact, during winter the mass balance curve is characterized by a slow increase followed by a fast and strong decrease during the summer period. Summing the solid precipitation (P_{solid}) with the ablation (M), the cumulative mass balance value (B) over the 4-year study period is −18.8 m (w.e.). Similar net mass balance values (−4.8 or −4.9 m w.e) were found in all years except 2007/2008 (−4.2 m w.e.).

Discussions

To assess the glacier ablation calculations from the energy fluxes, we compare the calculated ablation data to the measured values. The comparison is performed for a short but meaningful time frame during the summer season 2009 when some ablation stakes were located near the AWS1 Forni. On 24 July 2009 three ablation stakes were installed (according to the method introduced by Kaser et al., 2003). Measured ablation data from 24 July to 30 August 2009 are available for comparison with the values derived from the surface energy balance. The ablation amount at the stake locations was measured on 16 August 2009 and at the end of the period (on 30 August 2009). Two values for each stake can be compared to the calculated ice melting values (Table 4), and an ice density of 917 kg m^{-3} is used to convert observed mass balances in meter water equivalent. The comparison period we chose (from 24 July to 30 August 2009) has relatively low wind speed and no, or few, periods of negative air temperature (Fig. 3, parts a and b). Thus, it is not representative of the full range of conditions that

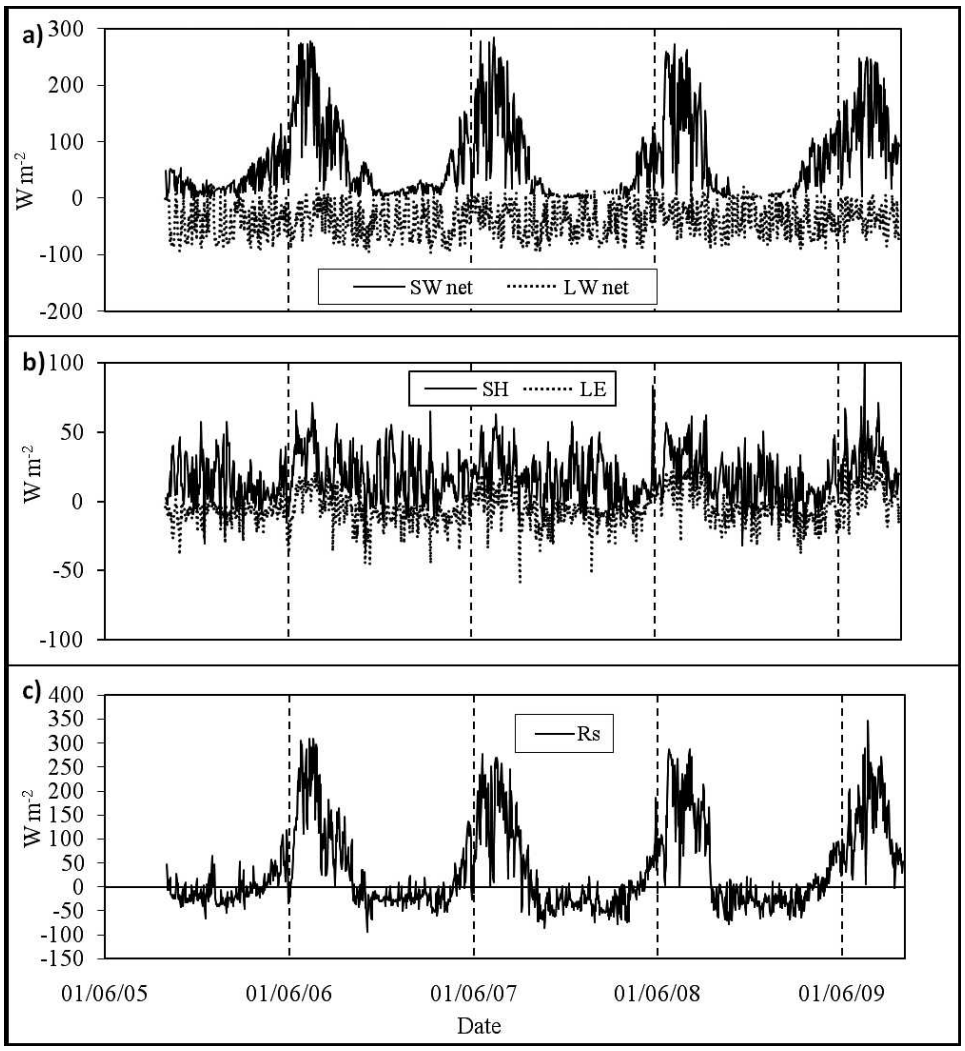

FIGURE 4. Components of the surface energy balance, showing daily mean values: (a) net shortwave and longwave radiation, (b) turbulent fluxes of sensible and latent heat, and (c) net energy available for ice/snow melting (please note the differences in vertical scales). The dates shown are dd/mm/yy.

may occur during the ablation season even if on the Forni Glacier summer days frequently show no negative air temperatures (Table 3) and the AWS site is characterized by low wind conditions. Nevertheless, our results demonstrate that the simple empirical calculation of the turbulent fluxes is valid and the heat conduction into snow/ice has little effect on total available melt energy.

Average measured melting is found to be −1.97 m w.e., compared to the −2.03 m w.e. of ice melting obtained from the energy balance calculation. In spite of the slight overestimation of melt from the energy balance, the two data sets are fairly well in agreement. In view of general errors involved in the measurements of ice ablation and radiation budget, the difference between calculated and observed values is rather small. In particular, the measured change of the glacier surface is a point measurement and not an accurate estimate of the mass loss in an area of 10 m × 10 m. Differences of several tens of centimeters easily develop during the ablation season between point measurements and nearby areas (Müller and Keeler, 1969). This is evident if ablation data collected from the three ablation stakes are compared and differences up to 20 cm can be found.

The availability of outgoing longwave radiation data permitted accurate calculation of the surface temperature and consequently the turbulent fluxes and surface energy balance. If no temperature sensor is installed at the glacier surface, T_S can be calculated from the outgoing longwave radiation flux, surface energy flux (e.g. Klok and Oerlemans, 2002) or air temperature (e.g. Oerlemans, 2000). Setting up surface temperature as a function of air temperature is incorrect, in particular when the surface energy balance is negative and measured air temperatures are positive, and also when air temperatures are <0 °C and Rs is positive. These inconsistencies have impacts on the outgoing longwave flux as well as the turbulent heat fluxes (Anslow et al, 2008). Consequently different methods impact the energy budget calculations. In our study on Forni Glacier, the turbulent heat fluxes are calculated from the LW_{out} data differently from Oerlemans (2000) on Morteratsch glacier, where the LW sensor was not available and T_S is calculated from the air temperature. Furthermore, in the present analysis, humidity, wind velocity, and air temperature are measured at >2 m at the AWS and then calculated at 2 m thus permitting us to estimate LE with more precision. In Klok and Oerlemans (2002) the turbulent fluxes calculations are different due to the absence of the wind sensor. The pattern of our energy balance values (Fig. 4) is in agreement with results from Klok and Oerlemans (2002) on Morteratsch Glacier rather than in Oerlemans (2000).

Table 1 shows a comparison between Forni and Morteratsch Glaciers, in particular the differences in AWS location and energy balance results reported. We refer to Oerlemans (2007) for the characteristics of the site. The Morteratsch data refer to annual mean values surveyed in 2000, except albedo (1995). Radiation and albedo values are similar, but greater differences are found

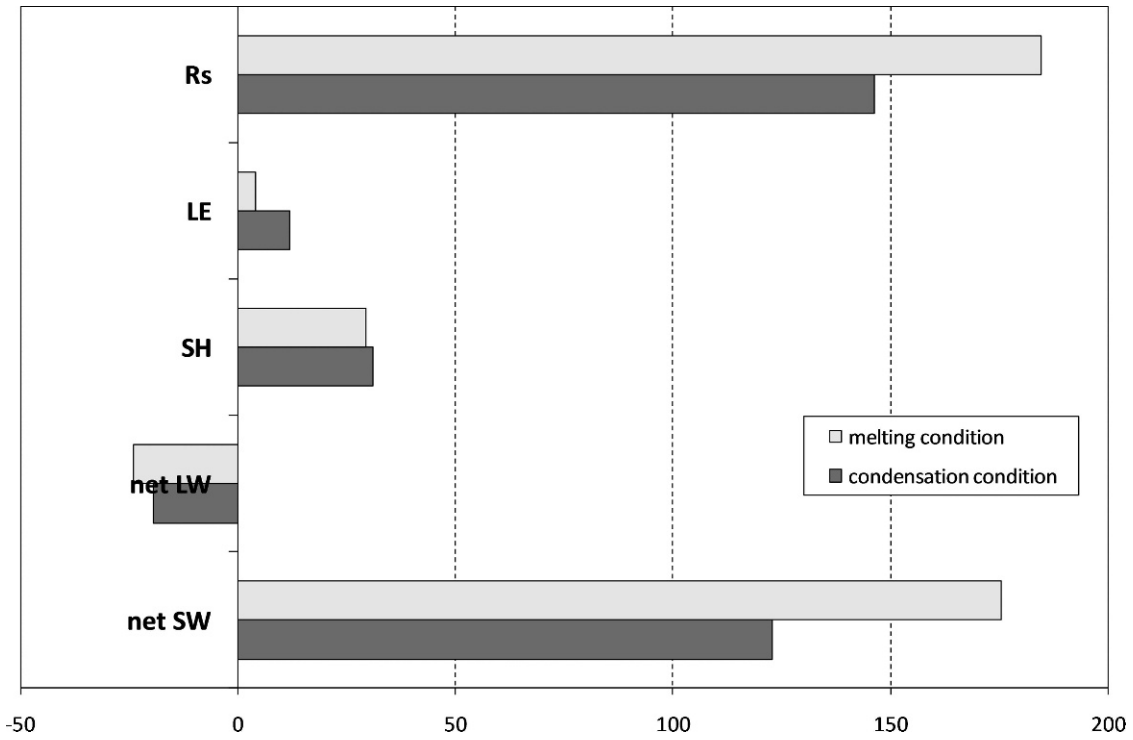

FIGURE 5. Components of the surface energy flux (from hourly mean values), averaged over time, when melting (i.e. about 31% of the time) (light gray) and condensation (i.e. about 24% of the time) (dark gray) conditions occurred. The units of measure for the *x*-axis are W m^{-2}.

between the turbulent fluxes: in particular SH and LE values on Forni are lower than on Morteratsch. The climatic setting of the two glaciers is the same, with Forni being a bit sunnier, then differences in air temperature and hence turbulent fluxes are simply due to the higher elevation of the Forni AWS.

In Table 3 we summarize the annual and seasonal values of the most important parameters for identifying the factors driving the 4-year glacier mass balance.

The mass balance values are more negative (-4.9 ± 0.022 m w.e.) during hydrological years 2005/2006 and 2006/2007, which

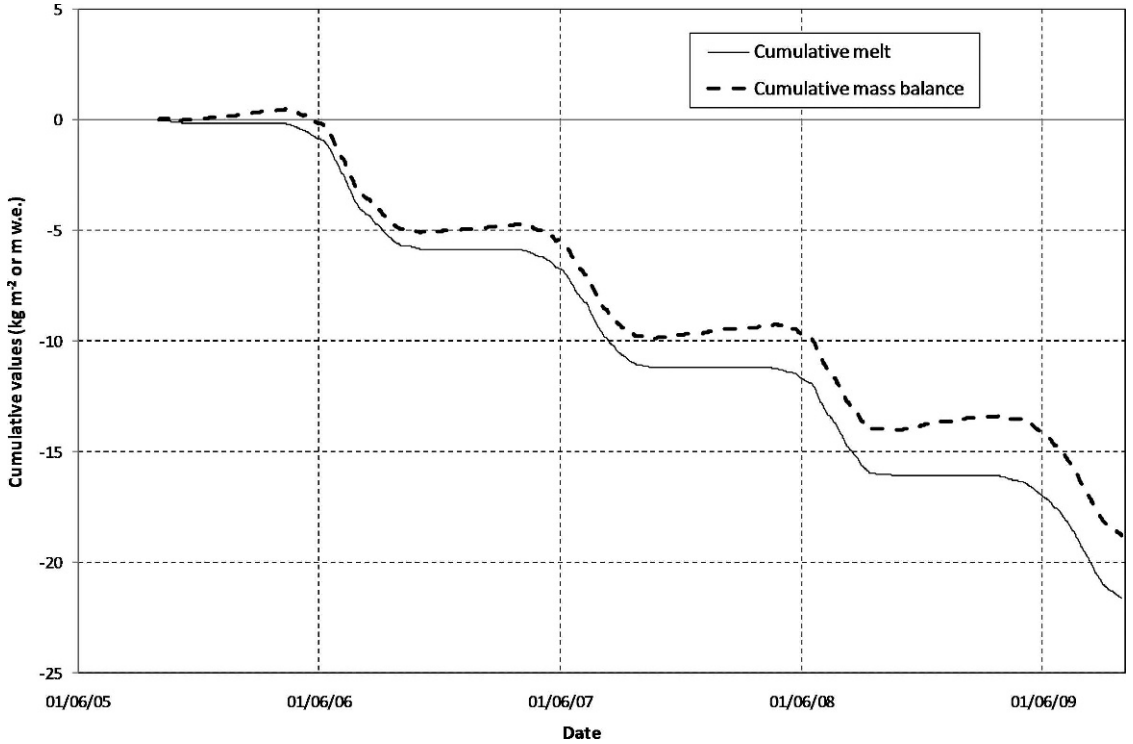

FIGURE 6. Cumulative melt (solid curve) and cumulative mass balance (dashed curve) calculated over the 4-year period. Values were obtained from hourly data analysis. The dates shown are dd/mm/yy.

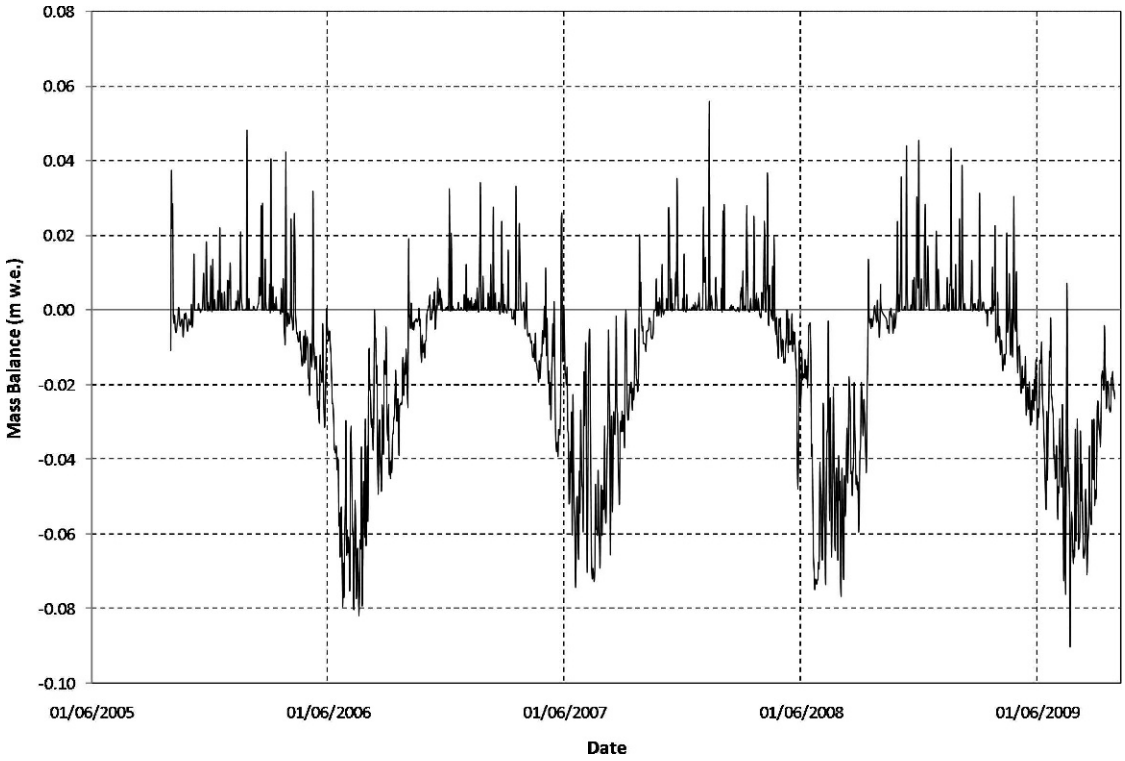

FIGURE 7. Point glacier mass balance calculated over the 4-year period: the daily total values obtained from hourly data analysis are shown. The dates shown are dd/mm/yyyy.

are both characterized by high melting values. During 2005/2006, the high mean energy balance and cumulative net shortwave radiation may have played an important role. Instead, 2006/2007 displays a fall season showing a positive mean energy balance, which seems to affect the trend of solid precipitation. In fact that year is characterized by the lowest snow accumulation (+0.6 ± 0.005 m w.e.). Differently, during 2007/2008, the cumulative mass balance is less negative (−4.2 ± 0.023 m w.e.) due to the lowest cumulative melt. That year is also characterized by the lowest mean energy balance and the lowest cumulative net shortwave radiation, and the snow accumulation corresponds to the 4-year mean value (+0.7 ± 0.006 m w.e.). During 2008/2009 the mass balance is lower than during 2005/2006 probably due to a slightly higher snow amount, even if cumulative melting presents the same value.

Concerning the annual and seasonal air temperature mean values (Table 3), a clear connection with the mass balance is not found. In fact, both the lowest mean air temperature values in 2005/2006 and the warmest ones in 2006/2007 correspond to a high cumulative melt. Instead, from our results the mass balance and melting amount appear more influenced by surface energy balance and surface conditions. Generally the albedo is very important in controlling magnitude and rates of snow and ice ablation. At the Forni AWS the mean summer albedo does not show strong changes during the analyzed period. The fall albedo displays a unique very low value in 2006/2007 (0.51) corresponding to a positive mean energy balance (18 W m^{-2}) and to a more negative cumulative melting. Also, spring albedo shows a single year (2007/2008) with a higher value (0.84) than all the other values, which vary between 0.76 and 0.78. The lowest melt occurs in the year with the highest spring albedo, in contrast to higher melt amounts found in periods with lower spring albedo.

The presence of fresh snow at the glacier surface reduces the adsorbed energy available for melting and also regulates the duration of the ice ablation season by delaying its start and/or anticipating the end. By analyzing the albedo and the snow cover trend (Fig. 3, last three panels) during the summer/fall seasons, we find for each year time frames characterized by ice albedo (i.e. from ca. 0.15 to ca. 0.4). Then the following ice ablation periods are found: 93 days in 2005/2006, 93 days in 2006/2007, 80 days in 2007/2008, and 90 days in 2008/2009. These results are in agreement with the mass balance budget; in fact, the summer/fall with the shortest period featuring ice albedo corresponds to the least negative melt and mass balance values (2007/2008). Longer time frames with glacier ice exposed to melt processes are found when stronger negative mass balance occurs (e.g. 2005/2006, 2006/2007).

TABLE 4

Measured and modeled ice melting (m w.e.) data at AWS1 Forni, using three ablation stakes (74, s1, and s2), in an area (50 m^2) around the AWS site (Fig. 1). An ice density of 917 kg m^{-3} is used to calculate melting (w. e.).

	Time frame*		
Data sources	from 24-07-09 to 16-08-09	from 16-08-09 to 30-08-09	from 24-07-09 to 30-08-09
Stake 74	−1.20	−0.71	−1.91
Stake s1	−1.27	−0.71	−1.98
Stake s2	−1.41	−0.61	−2.02
Average measured ice melting (w. e.)	−1.29	−0.68	−1.97
Calculated ice melting (w. e.)	−1.32	−0.71	−2.03

* All dates recorded as dd-mm-yy.

Then, from our analysis, surface conditions are crucial in determining the net energy available for ice melting, thus underlying the important role played by summer and fall solid precipitation, which changes glacier reflectivity even if in some cases only for short time frames. When the ice ablation season is characterized by frequent snowfall it corresponds to a minor adsorption of energy and then to a minor melt. Particularly important in determining the time length of the ice melt season are the duration of spring snow cover (whenever longer, it may postpone the start of ice melting) and the occurrence of earlier fall solid precipitation; the latter may anticipate the end of the ablation season. In fact, in 2007/2008 when the least negative melt is found, the end of the ablation season is marked by snowfall that occurred on 14 September. In other hydrological years, characterized by higher melt amount, the ablation season extends up to the end of September.

Summarizing the main factors driving the Forni Glacier mass balance are: snowfall events (especially during the ablation season), snow cover persistence, and albedo. A higher net cumulative shortwave radiation increases snow and ice melting, and consequently causes a lower albedo. Moreover, an albedo decrease could be also due to the debris present at the snow and ice surface (Nakawo and Young, 1982; Mihalcea et al., 2006; Flanner et al., 2009). In the case of Forni Glacier, a continuous debris cover is present only along the well developed medial moraines (Smiraglia, 1989), which are hundreds of meters distant from the AWS, thus making debris cover influence negligible at the AWS location. On the other hand, atmospheric soot (dust and black carbon) could also be responsible for decreasing the surface reflectivity of snow and then reducing its persistence. Dust and black carbon could be present at the glacier surface due to different causes including both natural sources and anthropogenic ones. The latter are linked to diesel combustion and deforestation. The natural sources can be from bacterial decomposition of organic matter (Takeuchi et al., 2001; Takeuchi, 2002; Fujita, 2007), fine sediments from moraines, from the Sahara (Sodemann et al., 2006), from fires, and from volcanic eruptions. Up to now no data are available for Italian glaciers describing atmospheric soot presence and then its role in driving surface albedo. On the Forni Glacier a pilot experiment is presently ongoing to collect snow samples for evaluating dust and black carbon presence (personal communication from P. Bonasoni, 2011). This could give us important information for describing glacier reflectivity evolution and then projecting future glacier melt under climate and atmospheric change scenarios.

Conclusions

The results obtained from AWS1 Forni during the 4-year period of data acquisition prove to be consistent with results from other AWSs located on the melting surface of other glaciers (i.e. the AWSs on Morteratschgletscher; see Oerlemans, 2000; Klok and Oerlemans, 2002).

The AWS1 Forni delivers a unique data set on meteorological conditions on a glacier snout in the Italian Alps. The data set (4 mass balance years) allows the study of the seasonal variation of surface energy fluxes. In particular, the complete surface energy balance was calculated at the AWS location, where radiative fluxes are known and non-radiative contributing factors (sensible and latent heat) can be calculated. Also the hourly scale analysis allows the calculation of surface ablation.

The complete energy balance analysis confirms that the parameter most influencing the surface net energy available for melting ice/snow (R_S) is the net shortwave radiation (SW_{net}) during melting ($T_S = 0$ °C and $R_S > 0$ W m^{-2}) and condensation ($T_S = 0$ °C and LE > 0 W m^{-2}) conditions. For a mean R_S value of 185 W m^{-2} (during melting) and 146 W m^{-2} (during condensation), mean SW_{net} is 176 W m^{-2} and 123 W m^{-2}, respectively; instead SH is ca. 30 W m^{-2} for both conditions, and LE was 4 W m^{-2} and 12 W m^{-2}, respectively. Therefore, non-radiative fluxes have less influence on ablation (during melting SH is ca. 16% and LE is ca. 2% of the R_S amount, and, during condensation, SH is ca. 21% and LE is ca. 8%).

These results are also supported by the comparison between field-measured and calculated ablation values during summer 2009, which shows only small differences mainly due to the ice surface ablation variability. Moreover, our results demonstrate that the simple empirical calculation of the turbulent fluxes is valid and the heat conduction into snow/ice has little effect on total available melt energy.

During the 4-year analysis, the total ice ablation calculated from the complete energy balance is -21.7 kg m^{-2} or m w.e., and the mass accumulation is +2.8 m w.e., thus giving a mass balance of -18.8 m w.e. The maximum melt is registered during 2005/2006 and 2008/2009 with an amount of -5.6 ± 0.020 m w.e., instead of the minimum during 2007/2008 (-5.0 ± 0.021 m w.e.). The year 2008/2009 is characterized by the highest accumulation ($+0.8 \pm 0.007$ m w.e.) and 2006/2007 by the smallest one ($+0.6 \pm 0.005$ m w.e.). The most negative mass balance is observed during 2005/2006 and 2006/2007 (-4.9 ± 0.023 and -4.9 ± 0.021, respectively), whereas the least negative value occurs during 2007/2008 (-4.2 ± 0.023 m w.e.).

Our findings suggest that the surface conditions, especially the role played by solid precipitation during summer and fall seasons, are important in determining the net energy available for ice melting. Particularly important are the permanence of spring snow cover (whenever longer, it may postpone the start of ice melting) and the occurrence of earlier solid precipitation during the fall season.

Glacier energy budget is also controlled by surface albedo. Its seasonal changes are driven by snowfalls and dust deposition. On this latter, the current literature (Flanner et al., 2009) suggests the possibility that atmospheric soot (dust and black carbon) is playing a role in driving the spring decrease of snow albedo also on Alpine glaciers' surfaces. Therefore the next step of our research will be to analyze with further details the glacier surface over a one-year period, also sampling snow and ice to find any correlations between surface reflectivity and atmospheric soot presence. Moreover we like to extend the computation of the glacier surface energy balance to the entire glacier basin.

Acknowledgments

We would like to thank the two anonymous reviewers for numerous helpful comments made on the first draft of the paper.

The AWS1 Forni project is developed under the umbrella of the SHARE Program. SHARE (Stations at High Altitude for Research on the Environment) is an international program developed and managed by the Ev-K2-CNR Committee. This work was conducted in the framework of the SHARE Stelvio project, promoted and funded by Ev-K2-CNR and Fondazione Lombardia per l'Ambiente; moreover, the data analysis was performed in the framework of the COFIN PRIN Project 2008.

We thank the Stelvio National Park, the Commune of Valfurva, the Valfurva section of the Italian Alpine Club (CAI), and the ARPA Lombardia for their kind help and support. We are also grateful to Gianpietro Verza, Eraldo Meraldi, and Roberto Chillemi for their fundamental technical assistance in the field.

References Cited

Ambach, W., 1963: Untersuchungen zum Energieumsatz in der Ablationzone des Grönländischen Inlandeises. *Meddelelser om Grønland*, 174: 4–311.

Anslow, F., Hostetler, S., Bidlake, W. R., and Clark, P. U., 2008: Distributed energy balance modeling of South Cascade Glacier, Washington and assessment of model uncertainty. *Journal Geophysical Research*, 113: F02019, doi:10.1029/2007JF000850.

Björnsson, H., 1972: Bæsigisarjökull, north Iceland. Results of glaciological investigations 1967–1968. Part II. The energy balance. *Jökull*, 22: 44–59.

Brock, B. W., Mihalcea, C., Kirkbride, M., Diolaiuti, G., Cutler, M., and Smiraglia, C., 2010: Meteorology and surface energy fluxes in the 2005–2007 ablation seasons at Miage debris-covered glacier, Mont Blanc Massif, Italian Alps. *Journal of Geophysical Research*, 115: D09106, doi:10.1029/2009JD013224.

Capello, C. F., 1959–1960: Ricerche di microclimatologia sulla superficie glaciale del Miage. *Bollettino del Comitato Glaciologico Italiano*, 9(II serie, parte prima): 95–154.

Citterio, M., Diolaiuti, G., Smiraglia, C., Verza, G., and Meraldi, E., 2007: Initial results from the Automatic Weather Station (AWS) on the ablation tongue of Forni Glacier (Upper Valtellina, Italy). *Geografia Fisica e Dinamica Quaternaria*, 30: 141–151.

Flanner, M. G., Zender, C. S., Hess, P. G., Mahowald, N. M., Painter, T. H., Ramanathan, V., and Rasch, P. J., 2009: Springtime warming and reduced snow cover from carbonaceous particles. *Atmospheric Chemistry and Physics*, 9: 2481–2497.

Fujita, K., 2007: Effect of dust event timing on glacier runoff: sensitivity analysis for a Tibetan glacier. *Hydrological Processes*, 21(21): 2892–2896.

Georges, C., and Kaser, G., 2002: Ventilated and unventilated air temperature measurements for glacier-climate studies on a tropical high mountain site. *Journal of Geophysical Research*, 107(D24): article 4775, doi:10.1029/2002JD002503.

Gregory, J. M., and Oerlemans, J., 1998: Simulated future sea-level rise due to glacier melt based on regionally and seasonally resolved temperature changes. *Nature*, 391(6666): 474–476.

Greuell, W., and Oerlemans, J., 1986: Sensitivity studies with a mass balance model including temperature profile calculations inside the glacier. *Zeitschrift für Gletscherkunde und Glazialgeologie*, 22(2): 101–124.

Greuell, W., Knap, W., and Smeets, P., 1997: Elevational changes in meteorological variables along a mid-latitude glacier during summer. *Journal of Geophysical Research*, 102(D22): 25941–25954.

Harrison, L. P., 1963: Fundamentals concepts and definitions relating to humidity. *In* Wexler, A. (ed.), *Humidity and Moisture*. New York: Reinhold Publishing Co., 3 pp.

Hock, R., 1999: A distributed temperature-index ice- and snowmelt model including potential direct solar radiation. *Journal of Glaciology*, 45(149): 101–111.

Hock, R., 2005: Glacier melt: a review on processes and their modelling. *Progress in Physical Geography*, 29(3): 362–391.

Hogg, I. G. G., Paren, J. G., and Timmis, R. J., 1982: Summer heat and ice balances on Hodges Glacier, South Georgia, Falkland Islands Dependencies. *Journal of Glaciology*, 28(99): 221–228.

Huss, M., Funk, M., and Ohmura, A., 2009: Strong alpine glacier melt in the 1940s due to enhanced solar radiation. *Geophysical Research Letters*, 36: L23501, doi:10.1029/2009GL0400789.

Ishikawa, N., Owens, I. F., and Sturman, A. P., 1992: Heat balance studies characteristics during fine periods on the lower parts of the Franz Josef Glacier, South Westland, New Zealand. *International Journal of Climatology*, 12: 397–410.

Kaser, G., Fountain, A., and Jansson, P., 2003: A manual for monitoring the mass balance of mountain glaciers. Paris, UNESCO, IHP, *Technical Documents in Hydrology*, 59 pp.

Klok, E. J., and Oerlemans, J., 2002: Model study of the spatial distribution of the energy and mass balance of Morteratschgletscher, Switzerland. *Journal of Glaciology*, 48(163): 505–518.

Klok, E. J., and Oerlemans, J., 2004: Modelled climate sensitivity of the mass balance of Morteratschgletscher and its dependence on albedo parameterization. *International Journal of Climatology*, 24: 231–245.

Mihalcea, C., Mayer, C., Diolaiuti, G., Lambrecht, A., Smiraglia, C., and Tartari, G., 2006: Ice ablation and meteorological conditions on the debris-covered area of Baltoro glacier, Karakoram, Pakistan. *Annals of Glaciology*, 43: 292–300.

Mölg, T., and Hardy, D. R., 2004: Ablation and associated energy balance of a horizontal glacier surface on Kilimanjaro. *Journal of Geophysical Research*, 109: D16104, doi:10.1029/2003JD004338.

Müller, F., and Keeler, C. M., 1969: Errors in short-term ablation measurements on melting ice surface. *Journal of Glaciology*, 8(52): 91–105.

Munro, D. S., 1989: Surface roughness and bulk heat transfer on a glacier: comparison with eddy correlation. *Journal of Glaciology*, 35(121): 343–348.

Munro, D. S., and Marosz-Wantuch, M., 2009: Modeling ablation on Place Glacier, British Columbia, from glacier and off-glacier data sets. *Arctic, Antarctic, and Alpine Research*, 41(2): 246–256.

Nakawo, M., and Young, G. J., 1982: Estimate of glacier ablation under a debris layer from surface temperature and meteorological variables. *Journal of Glaciology*, 28(98): 29–34.

Oerlemans, J., 2000: Analysis of a 3 year meteorological record from the ablation zone of Morteratschgletscher, Switzerland: energy and mass balance. *Journal of Glaciology*, 46(155): 571–579.

Oerlemans, J., 2001: *Glaciers and Climate Change*. Lisse: Balkema, 115 pp.

Oerlemans, J., 2007: Estimating response times of Vadret da Morteratsch, Vadret da Palü, Briksdalsbreen and Nigardsbreen from their length records. *Journal of Glaciology*, 53(182): 357–362.

Oerlemans, J., 2009: Retreating alpine glaciers: increased melt rates due to accumulation of dust (Vadret da Morteratsch, Switzerland). *Journal of Glaciology*, 55(192): 729–736.

Oerlemans, J., and Klok, E. J., 2002: Energy balance of a glacier surface: analysis of automatic weather station data from the Morteratschgletscher, Switzerland. *Arctic, Antarctic, and Alpine Research*, 34(4): 477–485.

Oerlemans, J., and Vugts, H. F., 1993: A meteorological experiment in the melting zone of the Greenland Ice Sheet. *Bulletin of the American Meteorological Society*, 74(3): 355–365.

Oerlemans, J., Anderson, B., Hubbard, A., Huybrechts, P., Jóhannesson, T., Knap, W. H., Schmeits, M., Stroeven, A. P., van de Wal, R. S. W., Wallinga, J., and Zuo, Z., 1998: Modelling the response of glaciers to climate warming. *Climate Dynamics*, 14(4): 267–274.

Oerlemans, J., Björnsson, H., Kuhn, M., Obleitner, F., Palsson, F., Smeets, P., Vugts, H. F., and De Wolde, J., 1999: Glacio-meteorological investigations on Vatnajökull, Iceland, summer 1996. *Boundary-Layer Meteorology*, 92: 3–26.

Oesch, D., Wunderle, S., and Hauser, A., 2002: Snow surface temperature from AVHRR as a proxy for snowmelt in the Alps. *Proceedings of EARSeL-LISSIG-Workshop Observing our Cryosphere from Space,* Bern, March 11–13, 2002, 163–169.

Oke, T. R., 1987: *Boundary Layer Climates.* 2nd edition. London: Routledge, 443 pp.

Paul, F., Escher-Vetter, H., and Machguth, H., 2009: Comparison of mass balances for Vernagtferner, Oetzal Alps, as obtained from direct measurements and distributed modeling. *Annals of Glaciology*, 50: 169–177.

Pellicciotti, F., Helbing, J., Rivera, A., Favier, V., Corripio, J., Araos, J., Sicart, J. E., and Carenzo, M., 2008: A study of the energy balance and melt regime on Juncal Norte Glacier, semi-

arid Andes of central Chile, using melt models of different complexity. *Hydrological Processes*, 22: 3980–3997.

Rupper, S., and Roe, G., 2008: Glacier changes and regional climate: a mass and energy balance approach. *Journal of Climate*, 21: 5384–5401.

Smiraglia, C., 1989: The medial moraines of Ghiacciaio dei Forni, Valtellina, Italy: morphology and sedimentology. *Journal of Glaciology*, 35(119): 81–84.

Smiraglia, C., 2003: Le ricerche di glaciologia e di morfologia glaciale in Italia. Evoluzione recente e ipotesi di tendenza. *In* Biancotti, A., and Motta, M. (eds.), *Risposta dei processi geomorfologici alle variazioni ambientali.* Atti del Convegno Conclusivo Programma MURST 1997, Bologna 10–11 February 2000, Brigati, Genova, 397–408.

Sodemann, H., Palmer, A. S., Schwierz, C., Schwikcowski, M., and Wernli, H., 2006: The transport history of two Saharan dust events archived in an Alpine ice core. *Atmospheric Chemistry and Physics*, 6(3): 667–688.

Takeuchi, N., 2002: Optical characteristics of cryoconite (surface dust) on glaciers: the relationship between light absorbency and the property of organic matter contained in the cryoconite. *Annals of Glaciology*, 34: 409–414.

Takeuchi, N., Kohshima, S., Shiraiwa, T., and Kubota, K., 2001: Characteristics of cryoconite (surface dust on glaciers) and surface albedo of Patagonia glacier, Tyndall Glacier, Southern Patagonia Icefield. *Bulletin of Glaciological Research*, 18: 65–69.

van den Broeke, M. R., 1997: Structure and diurnal variation of the atmospheric boundary layer over a mid-latitude glacier in summer. *Boundary-Layer Meteorology*, 83: 183–205.

van den Broeke, M. R., Duynkerke, P. G., and Henneken, E. A. C., 1994: Heat, momentum and moisture budgets of the katabatic layer over the melting zone of West Greenland ice sheet in summer. *Boundary-Layer Meteorology*, 71(4): 393–413.

von Hann, J., 1897: *Handbuch der Klimatologie*. Stuttgart, Germany: J. Engelhorn.

Wallinga, J., and van de Wal, R. S. W., 1998: Sensitivity of Rhonegletscher, Switzerland, to climate change: experiments with a one-dimensional flowline model. *Journal of Glaciology*, 44(147): 383–393.

Wexler, A., 1976: Vapor pressure formulation for water in the range 0° to 100°C—A revision. *Journal of Research of the National Bureau of Standards*, 80A: 775.

MS accepted July 2011